NASA TECHNICAL NOTE

NASA TN D-7697

NASA TN D-7697

FLOW MEASUREMENT IN BASE COOLING AIR PASSAGES OF A ROTATING TURBINE BLADE

by Curt H. Liebert and Frank G. Pollack

Lewis Research Center
Cleveland, Ohio 44135

NATIONAL AERONAUTICS AND SPACE ADMINISTRATION • WASHINGTON, D. C. • JUNE 1974

1 Report No.	2. Government Accession No.	3. Recipient's Catalog No.
NASA TN D-7697		

4. Title and Subtitle	5. Report Date
FLOW MEASUREMENT IN BASE COOLING AIR PASSAGES OF A ROTATING TURBINE BLADE	June 1974
	6. Performing Organization Code
7. Author(s)	8. Performing Organization Report No.
Curt H. Liebert and Frank G. Pollack	E-7886
	10. Work Unit No.
9. Performing Organization Name and Address	501-24
Lewis Research Center National Aeronautics and Space Administration Cleveland, Ohio 44135	11. Contract or Grant No.
	13. Type of Report and Period Covered
12. Sponsoring Agency Name and Address	Technical Note
National Aeronautics and Space Administration Washington, D.C. 20546	14. Sponsoring Agency Code

15. Supplementary Notes

16. Abstract

This report describes the operational performance of a shaft-mounted system for measuring the air mass flow rate in the base cooling passages of a rotating turbine blade. Shaft speeds of 0 to 9000 rpm, air mass flow rates of 0.0035 to 0.039 kg/sec (0.0077 to 0.085 lbm/sec), and blade air temperatures of 300 to 385 K (80° to 233° F) were measured. Comparisons of individual rotating blade flows and corresponding stationary supply orifice flows agreed to within 10 percent.

17. Key Words (Suggested by Author(s))	18. Distribution Statement
Flow characteristics; Rotational flow; Cooling systems; Measuring apparatus; Rotating fluids; Turbine cooling; Turbine blades	Unclassified - unlimited Category 14

19. Security Classif. (of this report)	20. Security Classif. (of this page)	21. No. of Pages	22. Price*
Unclassified	Unclassified	27	$3.25

* For sale by the National Technical Information Service, Springfield, Virginia 22151

FLOW MEASUREMENT IN BASE COOLING AIR PASSAGES OF A ROTATING TURBINE BLADE

by Curt H. Liebert and Frank G. Pollack

Lewis Research Center

SUMMARY

This report describes the operational performance of a shaft-mounted system for measuring the air mass flow rate in the base cooling passages of a rotating turbine blade. Total and static pressures were sensed in the blade base coolant passages. The sensed pressures were ducted to variable reluctance differential pressure transducers mounted near the shaft centerline. These rotating transducers converted the pneumatic pressures into electrical signals that were transferred by a slip ring assembly to stationary recording equipment. The pressure differences indicated by the transducers were corrected for temperature, rotational effects on the air columns contained by the ducting and, when relevant, rotational effects on the transducers. Mass flow rates were calculated from these corrected pressure differences. Shaft speeds of 0 to 9000 rpm, air mass flow rates of 0.0035 to 0.039 kilogram per second (0.0077 to 0.085 lbm/sec), and blade air temperatures of 300 to 385 K (80° to 233° F) were measured. Comparisons of individual rotating blade flows and corresponding stationary supply orifice flows agreed to within 10 percent.

INTRODUCTION

This report describes the results of an experimental investigation of a shaft-mounted system for measuring the mass flow rate of air through the coolant passages of a rotating turbine blade. The investigation was made principally on a rotating blade assembly in a cold-air spin rig that geometrically simulated the turbine blade and disk components of a cooled turbine from an aircraft engine.

Current methods for determining cooling air mass flow rates through rotating gas turbine blades use instrumentation located in a stationary portion of the blade coolant supply system. Coolant system leakages which may occur downstream of the measuring

station are accounted for through use of calibrations and calculations. While it is usually possible to calibrate and/or calculate the coolant system leakage at cold stationary conditions, it is not possible to apply such procedures with a high degree of confidence when the turbine component is hot and rotating. Therefore, to obtain an accurate determination of the coolant flow rate being delivered to a rotating cooled turbine blade it is desirable to make flow measurements at a point which is downstream of all potential points of coolant system leakage. A logical location for making such flow measurements is in the blade base airflow passages. The geometry of many present day air-cooled blades is such that pressure instrumentation can be installed in these air flow passages for the purpose of determining mass flow rates.

The purpose of the presently reported investigation was to determine the feasability of obtaining rotating cooling air flow measurements within the base coolant passages of a turbine blade. A modified version of the rotating pressure transfer system developed in reference 1 was used to permit the required pressure measurements made on the rotating blade to be transferred to stationary recording instruments.

The cold spin rig tests were made at shaft speeds from 0 to 9000 rpm, at blade cooling airflow rates ranging from about 0.0035 to 0.039 kilogram per second (0.0077 to 0.085 lbm/sec), and at blade cooling air temperatures that ranged from 300 to 385 K (80° to 233° F). These shaft speeds and cooling air conditions partially simulated the environmental conditions for a rotating air-cooled blade in a gas turbine engine.

SYMBOLS

a cooling air passage area

c_p specific heat at constant pressure

p pressure

R gas constant for air

r radius

T temperature

V velocity

$\dot{w}$ cooling air mass flow rate

α calibrated effective area

γ ratio of heat capacity at constant pressure to heat capacity at constant volume

ω angular velocity

Subscripts:

A	arbitrary radial location, such that $r_A > r_B$ (eq. (1))
amb	ambient pressure adjacent to rotary instrumentation (fig. 8(a))
B	arbitrary radial location, such that $r_A > r_B$ (eq. (1))
b	blade
o	calibrated orifice
s	static conditions
t	total conditions
1, 2, 3, 4, 5, 6	specific radial locations (fig. 8)
I, II	blade base cooling air passages (fig. 7)

APPARATUS

The items of test apparatus used in this experimental investigation were chosen to simulate the cooling airflow path and/or to partially simulate the environmental conditions for a rotating air-cooled blade in the research gas turbine engine of reference 2. This choice was deliberate because the pressure measuring system was being developed for future use on this engine. The test apparatus consisted of two blade assemblies, a bench-type flow calibration rig and a cold air spin rig with attached shaft air seal assembly and rotary instrumentation package. Detailed descriptions of these items are given in the following paragraphs.

Blade Assemblies

The air-cooled turbine blade that was used in this experimental investigation was from the research engine described in reference 2. The same blade (with the same pressure instrumentation installed in the blade base) was used throughout this investigation; however, this blade was adapted in turn to different air supply ducts for stationary flow tests (bench-type flow calibration tests) and rotating flow tests (spin rig tests). Figure 1 shows the blade assembly for the stationary bench flow tests and figure 2 shows the blade assembly for the spin rig tests. The blade had a simple radial throughflow cooling configuration. Cooling air entered the bottom of the base below the mounting serrations, and flowed radially outward and exited at the tip.

Bench flow tests. - The assembly of the blade and the cooling air supply duct for the

stationary bench flow tests is shown in figure 1. The duct configuration partially simulated the geometry of the cooling airflow path on the research engine of reference 2. The duct was soldered to the base of the blade (fig. 1); the supply end of the duct (on the right in fig. 1) was provided with a fitting for attachment to the bench flow calibration rig. A sound-deadening exhaust duct was soldered to the blade tip and connected to a laboratory exhaust system.

Spin rig tests. - The assembly of blade and cooling air supply duct for the spin rig tests is shown in figure 2. This ducting closely simulated the geometry of the air passage of the research engine (ref. 2) and was welded to the blade base. The lower end of the air supply duct was flanged to mate with a hollow stub shaft attached to the spin rig.

Bench Flow Calibration Rig

The bench flow calibration rig was a permanent part of the flow calibration equipment at the Lewis Research Center. This rig contained a standard, accurately calibrated orifice for determination of airflow.

Spin Rig and Attached Components

The spin rig, with the shaft air seal assembly and the rotary instrumentation package attached, is shown in figures 3 and 4.

Cold air spin rig. - The disk and shaft of the cold-air spin rig were driven by an air turbine (not shown in figs. 3 and 4). The disk contained fir-tree serrations on the rim for mounting turbine blades. The radial position and tip speed of the blade in the research engine of reference 2 could be simulated in the spin rig. A protective cover (shown in phantom in fig. 4) enclosed the disk. The top half of this cover is shown in the opened position in figure 3. For purposes of this investigation, the spin rig blade assembly was mounted on the disk, the shaft air seal assembly was mounted around a hollow stub shaft attached to the hub of the disk and the rotary instrumentation package was coupled to the right end of the stub shaft as shown in figures 3 and 4.

Shaft air seal assembly. - To provide for an effective comparison of airflow measurements made in the blade with airflow measurements made with an orifice mounted in a stationary air supply line, a virtually leak-free sealing arrangement was essential at the point where the cooling air was transferred from the stationary to the rotating part of the spin rig air supply system. Such a seal is shown schematically in figure 5. (The seal is also shown in less detail in figs. 3 and 4.) This seal was designed espe-

cially for this investigation. The entire shaft air seal assembly was stationary and the assembly was supported by the protective cover of the spin rig.

Blade cooling air (heavy arrows in fig. 5) supplied from a laboratory air system flowed into an inlet duct in the stationary seal assembly and then entered an annular passage in the stub shaft through holes in the stub shaft wall. Commercial segmented carbon ring shaft seals that rubbed on the outer diameter of the hollow stub shaft minimized leakage of cooling air along the shaft.

Radial and axial pressures on the carbon rings were applied by springs internal to the seal housing. Pins press-fitted into the housing held these rings stationary. The seals were designed to seal gases unidirectionally with the high pressure side of the seal located adjacent to the cooling air flow. The seals were designed to operate to pressures of 1.03×10^7 N/m^2 (1500 psi) over a temperature range of 22 to 589 K (-420° to 600° F). To ensure minimal blade cooling air leakage across the seals, buffer air was applied to the low pressure side of the shaft seal (thin arrows, fig. 5). The quantity of air used to maintain the buffer pressure was minimized by use of labyrinth seals mounted in the stationary seal assembly.

Modified rotary pressure transfer system. - The rotary pressure measuring system described in reference 1 was modified to transfer both rotating pressure and temperature signals to stationary data recording equipment for this experimental investigation. This rotary instrumentation package is shown photographically in figure 3 and schematically in figure 4. The package consisted of a stationary outer housing (shown in phantom in fig. 4), a rotating transducer compartment containing four variable reluctance differential pressure transducers and a 13-channel mercury slip ring assembly. The transducers converted pneumatic pressures from rotating pressure taps in the blade into electrical signals. A complete description of the transducers is given in reference 1. The slip ring assembly transferred these electrical signals from the rotating transducers to stationary signal conditioning and data recording equipment and also transferred excitation voltage from a stationary power supply to the rotating transducers. The slip ring assembly was also used to transfer thermocouple signals from the rotating parts to stationary recording equipment. For the purpose of this investigation, only four pressure transducers (representing four slip ring channels) were used in the rotary instrumentation package; the other channels on the 13-ring slip ring assembly were used for three rotating thermocouples (six channels), pressure transducer input power supply (two channels) and a common ground or the pressure transducers (one channel). A block diagram of the rotating pressure and temperature measurement system is shown in figure 6.

INSTRUMENTATION

Cooling air pressure and temperature measurements were made in the supply line and in the blade assemblies during both the bench flow tests and the spin rig tests to determine mass flow rates. During the spin rig test, measurements of shaft speed, spin rig and instrumentation package vibrations, pressure tubing and pressure transducer metal temperatures, and ambient air environmental temperatures were also made. Details of this instrumentation are given next.

Stationary Instrumentation

Bench flow tests. - The pressure and temperature sensors at the orifice in the cooling air supply line for the bench flow tests were an integral part of the flow calibration rig. The sensed pressures were measured with transducers; the sensed temperatures were read on precision gages.

The nature and location of the pressure instrumentation on the blade during the bench flow tests are shown in figure 7. The cooling air temperature was measured with a thermocouple (not shown) located just upstream of the cooling air supply duct shown in figure 1. A total pressure probe and a wall static pressure tap were installed in each of the two blade base cooling air passages.

The 0.051-centimeter- (0.020-in.-) diameter static taps were sharp edged, burr-free and normal to the inside of the blade base air passage. The outer surface of the blade base was counter-bored at each static tap location to accept a connecting lead of stainless steel tubing which was silver soldered to the blade base.

The total pressure probes were fabricated from 0.0813-centimeter- (0.032-in.-) diameter stainless steel tubing with a wall thickness of 0.0152 centimeter (0.006 in.). Two holes, 0.051 centimeter (0.020 in.) in diameter with hole centers spaced 0.127 centimeter (0.050 in.) apart, were drilled into each tube to form total pressure taps as shown in figure 7. After drilling, the tube end was sealed. Holes were drilled through the sides of the blade base into each air passage to accommodate the total pressure probes. These holes were located such that the probes were centered in the air flow passage (see fig. 7) and were in the same plane as the static wall taps. The completed pressure probes were inserted into the blade base, carefully alined so that the holes in the probes faced upstream and were equidistant from the walls of the passage. After insertion, the probes were silver soldered in place. All pressure leads were connected to water and mercury manometers for the bench flow tests.

Spin rig tests. - Static pressure taps and a thermocouple were used with the calibrated orifice in the stationary cooling air supply line during the spin rig tests to pro-

vide measurements for mass flow determination. Stationary thermocouples were used to monitor the temperature of the air space enclosed by the spin rig protective cover. These thermocouples were at radii of 7.62 and 26.7 centimeters (3 and 10.5 in.) and were about 5.08 and 0.76 centimeters (2 and 0.30 in.), respectively, from the face of the turbine disk (fig. 4). A stationary thermocouple was located 0.635 centimeter (0.25 in.) from the face of the cold junction reference block on the rotary instrumentation package (fig. 4) to monitor the reference temperature. Ambient pressure adjacent to the rotary instrumentation package was measured with a barometer. The spin rig shaft speed was measured with a magnetic pickup and the vibration levels on the spin rig and rotary instrumentation package were measured with displacement amplitude pickups.

During nonrotating pressure calibration tests on the pressure difference transducers in the spin rig (described later), the calibration pressure was measured on precision pressure gages calibrated to 0.25 percent of the full-scale reading associated with the range of the transducers used herein. Voltage output on the transducers was recorded through the system shown schematically on figure 6. The accuracy of the signal conditioning and recording was 1 percent of full scale.

Rotating Instrumentation

The pressure instrumentation (fig. 7) described for the bench flow test blade assembly (fig. 1) was used intact to measure pressure on the rotating blade assembly (fig. 2) during the spin rig tests. However, in the spin rig tests, the pressure leads were extended to permit connection with the pressure transducers in the rotary instrumentation package.

Figure 2 shows the static and total pressure tubing leads. After the blade assembly was installed on the disk, these tubing leads were secured to the blade base and disk with spot-welded straps and epoxy. Additional tubing was soldered to each lead to provide sufficient length to extend down the face of the disk, through the hollow stub shaft and hollow shaft coupling to the pressure transducers located in the rotary instrumentation package. This additional tubing was also secured to the rotor with straps and epoxy.

Total-static and total-ambient pressure differences were measured in each passage of the blade base by using the instrumentation described previously. Figure 8 shows schematically the location of the instrumentation in the spin rig tests. The total-ambient pressure difference (fig. 8(a)) was measured by attaching a total pressure lead from the blade base coolant passage to a port on one side of a differential pressure transducer and connecting the other port to a tube which extended along the centerline of the hollow shaft to the outside of the rotary instrumentation package. The total-static

pressure difference (fig. 8(b)) was obtained by attaching a static pressure lead from the blade to a port on one side of a differential pressure transducer and attaching a total pressure tube to a port corresponding to the other side of the same transducer. Transducers of 0 to 6.89×10^4 N/m^2 (0 to 10 psid) range were used to measure the total-static pressure differences, and transducers of 0 to 6.89×10^5 N/m^2 (0 to 100 psid) range were used to measure the total-ambient pressure differences.

One rotating thermocouple was mounted near the base coolant passage inlets in the blade cooling air supply duct (figs. 4 and 7), another was attached to the pressure sensing tubing on the disk T_6, and a third was installed immediately adjacent to a transducer mounted in the rotating transducer compartment (fig. 4). The positions of these three thermocouples are shown in figure 4. The pressure tubing thermocouple was placed 15.24 centimeters (6 in.) from the shaft centerline. Leads from the air supply duct and pressure tubing thermocouples were secured to the disk with spot-welded straps and epoxy. These leads extended through the stub shaft and coupling to the rotary instrumentation package in the same routing that was used for the pressure leads.

PROCEDURE

Calculation Procedure

Rotating pressures. - Measurement of the coolant flow rates in the base coolant flow passages of the rotating blade depended on the determination of the total and static pressure at this location during rotation. Because the pressure taps in the blade base that sensed these pressures and the differential pressure transducers in the rotary instrumentation package that reacted to these sensed pressures were at different radii, the indicated transducer pressure differences had to be corrected for rotational effects, including any density changes in the radial pressure leads due to temperature variations imposed on these leads. The following equation for making this correction was obtained from reference 1. (All symbols are defined in the appendix.)

$$p_A = p_B \exp\left[\frac{\omega^2\left(r_A^2 - r_B^2\right)}{2RT}\right] \tag{1}$$

This relation (derived from a model which predicts the centrifugal force (pressure) on air columns in the tubes) incorporates the following assumptions: a one-dimensional balance of forces on the radial air columns (pressure tubing leads) connecting any two

arbitrary radial points A and B, no temperature gradient along these air columns, constant column cross-sectional areas, and applicability of the perfect gas law.

Equation (1) was used in a two-step correction procedure to calculate the total pressure in each blade base passage during rotation. The instrumentation schematic on figure 8(a) shows the relation between the various locations involved in this procedure. For the first step, point A was taken at the reference pressure port of the transducer ($p_A = p_1$; $r_A = 2.86$ cm (1.125 in.)), point B was taken at the shaft centerline where the pressure is ambient ($p_B = p_{amb}$; $r_B = 0$) and T was assumed to be the temperature T_5 of the reference pressure lead as measured by the stationary thermocouple in the rotary instrumentation package (shown in figs. 4 and 8(a)). The value of p_1 was determined by substituting these values into equation (1). Next, p_2 was calculated by using the measured transducer pressure difference $p_2 - p_1$ and the calculated value of p_1. For the second correction step, point A was taken at the total pressure tap in the blade base ($p_A = p_t$; $r_A = 28.73$ cm (11.31 in.)). Point B was taken at the transducer port which was connected to the total pressure sensing lead ($p_B = p_2$; $r_B = 2.86$ cm (1.125 in.)) and T was assumed to be the temperature T_6 of the entire length of the pressure leads as measured by the thermocouple attached to the leads on the face of the turbine disk. Substituting these values into equation (1), the value of p_t was determined.

Equation (1) and the geometrical relation of the pressures from the centerline shown schematically in figure 8(b) were used to correct the indicated total-static pressure difference $p_4 - p_3$ to the actual pressure difference, $p_t - p_s$ in each blade base passage during rotation. Because p_t and p_s were measured at the same radius ($r_t = r_s$) and the temperatures of the pressure leads for the two measurements were the same (i.e., $T = T_6$), equation (1) may be written as

$$p_t - p_s = (p_4 - p_3) \exp\left\{\frac{\omega^2\left[(r_t)^2 - (r_4)^2\right]}{2RT_6}\right\} \tag{2}$$

Orifice cooling air mass flows. - The mass flows of cooling air through the orifices $\dot{w}_o$ in both the bench flow tests and the spin rig tests were determined from the orifice characteristics and the pressure and temperature measurements at the respective orifices. The inaccuracy of these mass flows is ±1/2 percent of full scale.

Blade cooling air mass flows. - Calculation of the mass flow rate through each of the blade base cooling air passages was accomplished for both the bench flow tests and the spin rig tests using the basic flow equation

$$\dot{w} = \frac{p_s Va}{RT_s} \tag{3}$$

Total flow through the two passages in the blade base (figs. 4 and 7) could be expressed as

$$\dot{w}_b = \left(\frac{p_s V a}{R T_s}\right)_I + \left(\frac{p_s V a}{R T_s}\right)_{II} \tag{4}$$

Values of velocity V in the passages were determined from the relation

$$V = \left\{ 2 c_p T_t \left[1 - \left(\frac{p_s}{p_t}\right)^{(\gamma-1)/\gamma} \right] \right\}^{1/2} \tag{5}$$

where $T_t = T_s$ was the steady-state temperature of the cooling air measured by the thermocouple (figs. 4 and 7) in the blade cooling air supply duct. The values of c_p and γ (corresponding to T_s) were taken from reference 3. The values of p_t and p_s were calculated as described previously for the rotating spin rig test; these values were measured directly during the bench-type flow calibration tests and the stationary spin rig tests.

Direct measurement of the cooling passage area a was not practical; nor was it practical to determine the effects of the nonideal right angle turns in the flow path immediately upstream of the blade base instrumentation plane (figs. 4 and 7) on the quantitative values of the measured total and static pressures. Therefore to compensate for these unknown values, calibrated effective areas α_I and α_{II} were substituted for the actual areas a_I and a_{II}, in equation (4). It was further assumed that $\alpha_I = \alpha_{II} = \alpha$ and that $T_{s,I} = T_{s,II} = T_s$. Thus equation (4) was rewritten as

$$\dot{w}_b = \frac{\alpha}{R T_s} \left[(p_s V)_I + (P_s V)_{II} \right] \tag{6}$$

An iterative procedure was used to determine the value of α for this blade from the bench flow test data. For an assumed value of α, $\dot{w}_b$ was calculated for each test point using equation (6). The calculated values of $\dot{w}_b$ were plotted against measured values of the supply air mass flow rate measured at the calibrated orifice $\dot{w}_o$, and a linear least-square fit was applied to these data. Iteration on α was continued until the slope of the least-square line passing through the origin was unity.

Operating Procedure

Bench flow tests. - This test to determine the value of α was made on the blade assembly shown in figure 1 using the bench flow calibration rig previously described. Cooling air flowed through the bench flow calibration rig and then through the blade assembly. For each flow setting, the total and static pressure in the blade base, cooling air temperature, orifice pressures and temperatures were recorded. A range of orifice cooling air mass flows from 0.00490 to 0.064 kilogram per second (0.0108 to 0.141 lbm/sec) was covered.

Shaft air seal system leakage check. - Leakage of cooling air from the shaft air seal system was checked with and without shaft rotation. At zero shaft speed, the leakage check was done at a high coolant airflow rate with no buffer airflow. A commercial leak-check fluid was applied to the outboard labyrinth fingers and the seal assembly was observed visually to detect leakage.

At shaft speeds of 4000 and 9000 rpm, numerical comparisons were made of the measured orifice flow $\dot{w}_o$ and the calculated blade flow $\dot{w}_b$ for various cooling airflow rates and for various pressure differences between cooling air and buffer air. Leakage of cooling air through the seal would be indicated by a difference between these two flow rates that changed progressively with increase in cooling-buffer air pressure difference. At 4000 rpm, a constant cooling airflow rate of 0.02 kilogram per second (0.044 lbm/sec) was used; at 9000 rpm, cooling airflow rates of 0.01, 0.02, 0.03, and 0.040 kilogram per second (0.022, 0.044, 0.066, and 0.088 lbm/sec) were used. At both speeds, cooling-buffer air pressure differences of about 228, 4964, and 13 650 N/m^2 (0.033, 0.72, and 1.98 psid) were used at each cooling airflow rate.

Transducer calibration. - All differential pressure transducers used in this investigation were calibrated under nonrotating conditions while mounted in the rotary instrumentation package on the spin rig. In addition, the two lower range differential pressure transducers measuring total-static pressure differences were calibrated for zero shift (change in output voltage with zero pressure difference applied to the transducers) with rotational speed.

Special calibration ports on the instrumentation package permitted external pressurization of the transducers independent of the pressure sensing lead system while the shaft was not rotating. Using these calibration ports, known pressures were applied to both ports of each transducer to cover the pressure difference ranges that would be used during the course of this investigation. These ranges were 0 to 6.89×10^4 N/m^2 (0 to 10 psid) pressure difference for the total-static pressure difference transducers and 0 to 6.89×10^5 N/m^2 (0 to 100 psid) pressure difference for the total-ambient pressure difference transducers. A number of discrete transducer temperatures between 300 and 370 K (80° and 206° F) were imposed on the transducers during this stationary calibration testing. The voltage outputs of the individual transducers were recorded and

plotted for each combination of pressure difference and temperature conditions. To determine the quality of the transducers, values of the commonly used performance characteristics (linearity and hysteresis) described in detail in reference 1 were determined from these transducer calibrations made at zero rig shaft speed.

Rotating calibration tests described in reference 1 showed that, at constant transducer temperature, transducer zero shift could vary with rotational speed for transducers of the 0 to 6.89×10^4 N/m^2 (0 to 10 psid) pressure difference range. Transducers of this range were used in this investigation to measure the total-static pressure differences. The 0 to 6.89×10^5 N/m^2 (0 to 100 psid) transducers used to measure the total-ambient pressure differences in this investigation had heavy diaphragms that were considered to be negligibly susceptible to distortion and rotational zero shift at the g-forces encountered. Therefore, it was assumed that these transducers had no constant-temperature zero shift with rotation and rotating calibrations were limited to the lower range transducers.

For the rotating calibration tests on the total-static pressure difference transducers, it was not possible to make use of the aforementioned calibration ports. For these tests, the cooling air and buffer air supply lines were closed. With no cooling airflow, the air column in the blade base was essentially stagnant except for some natural convection flow due to pumping and frictional heating. This situation resulted in a negligible pressure difference on the transducer because the total and static air pressures in the blade base were essentially equal. Transducer temperature could be held at a constant value of 340 K (152° F) at shaft speeds up to 1000 rpm only; above this speed, frictional heating in the adjacent air chambers caused the transducer temperatures to rise with shaft speed to a maximum temperature of 370 K (206° F) at 9000 rpm. Accordingly, calibration tests were made on the transducers at speeds of 0, 400, 600, and 1000 rpm and at constant transducer temperature of 340 K (152° F). In the range from 1000 to 9000 rpm, (where transducer temperatures exceed the 340 K (152° F) level), the recorded zero pressure difference output voltages were corrected to the constant 340 K (152° F) temperature level by adding or subtracting a millivolt value equal to the zero shift for that transducer at the equivalent temperature under conditions of no rotation. This method of correcting output voltages was based on the assumption that the zero shift due to rotation and zero shift due to temperature were additive but completely independent of each other. Any variation of the zero pressure difference output millivolts for zero shaft speed from the zero pressure difference output millivolts at some nonzero shaft speed as adjusted by the aforementioned temperature correction was assumed to be due to a zero-shift caused by rotation.

Spin rig tests. - Steady-state rotating cooling air mass flow tests on the blade were conducted with the blade assembly (fig. 2), the spin rig, the shaft air seal assembly, and the rotary instrumentation package in the configuration shown in figure 4. For all

spin rig testing (except the shaft air seal assembly leakage tests described previously) the cooling air-buffer air pressure difference was held at a constant value of 248 N/m^2 (0.036 psi). Combinations of shaft speeds and cooling airflow rates were chosen in a random fashion to cover a shaft speed range of 0 to 9000 rpm and a cooling airflow range of 0.0035 to 0.039 kilogram per second (0.0077 to 0.085 lbm/sec). Pressures and temperatures associated with the cooling airflow measurements were recorded for each test point. In addition, vibration, bearing temperature, and oil temperature measurements on the spin rig and the rotary instrumentation package were monitored.

RESULTS AND DISCUSSION

Bench Flow Tests

The value of the calibrated effective area α was determined from the bench flow test data by correlating orifice flow $\dot{w}_o$ and blade flow $\dot{w}_b$ using the iterative calculation procedure previously described. Figure 9 shows that, on the basis of 47 data points covering minimum to maximum flow rates, α was determined to be 0.316 square centimeter (0.0490 $in.^2$). The maximum deviation from the correlation line for an individual data point was about ±3 percent.

Shaft Air Seal Assembly Leakage Check

No leakage was apparent during the stationary shaft air seal leakage check with a leak detection fluid. The data taken during the rotating leakage check did not indicate any trend of increasing flow differences $\dot{w}_o - \dot{w}_b$ with increasing cooling air-buffer air pressure differences; values of $\dot{w}_b$ agreed with values of $\dot{w}_o$ within ±9 percent over the full range of leakage check tests. The shaft seal leakage was also calculated by the method of reference 4. Using the maximum cooling-buffer air pressure difference, 13 650 N/m^2 (1.98 psid), negligibly small leakages on the order of 10^{-5} kilogram per second (2.2×10^{-5} lbm/sec) were predicted. It was therefore concluded that the shaft air seal assembly could be assumed to be leakage free under all operating conditions.

Transducer Calibration Tests

The transducer calibrations of millivolt output as a function of applied pressure difference at discrete temperature levels determined from the stationary calibration tests in the spin rig were the basis for evaluating the rotational effect on the pressure differ-

ence transducers. The data from the zero pressure difference rotating calibration tests on the 0 to 6.89×10^4 N/m^2 (0 to 10 psid) pressure difference range transducers were analyzed as zero-shift (mV) as a function of shaft speed (rpm) after being adjusted for temperature effect. For these two total-static pressure difference transducers there was a small linear increase of zero-shift with speed over the range from 0 to 9000 rpm. (The calculated value of $\dot{w}_b$ could have been as much as 3 percent low if zero shift as a function of speed had not been taken into account.) This linear characteristic of the transducers was also noted in reference 1.

Spin Rig Flow Tests

The performance data for the rotating flow measuring system in the cold spin rig where typical engine speeds, cooling airflow rates, and cooling air pressure levels were investigated are shown in figure 10. The data are presented on the same basis that was used to present the bench flow test data (i.e., blade airflow rate $\dot{w}_b$ as a function of orifice airflow rate $\dot{w}_o$). In preparing this data plot, the value of 0.316 square centimeter (0.0490 in.^{2}) for the calibrated effective area α, that was previously determined for the bench flow test data, was used in equation (6). Sixty-seven spin rig test points recorded over a speed range from 0 to 9000 rpm, a cooling airflow range of 0.0035 to 0.039 kilogram per second (0.0077 to 0.085 lbm/sec), and a cooling air temperature range of 300 to 385 K (80° to 233° F), are shown in figure 10. A least-squares line fit of these data points produced a correlation line of $\dot{w}_b = \dot{w}_o$. The maximum data scatter about this correlation line was ±10 percent.

Before this experiment was performed, it was not obvious that the accuracy of the flow measurements made in the base airflow passages of the blade would not be seriously affected by the very disturbed flow conditions which could occur at the pressure measurement station. When the blade was not rotating, these disturbances may arise because the flow was turbulent and because the pressure measurement station was located immediately downstream of two right angle turns in the flow channels (see fig. 4). These turns can cause flow stream eddies; and the combination of turbulence and eddies could cause irregular pressure fluctuations (ref. 5) which may result in uncertainties in the values of $\dot{w}_b$ calculated with equations (1) to (6). When the blade is rotating, the additional effects of centrifugal forces on the coolant airflow could further disturb the flow (ref. 6). The good correlation (±3 percent) between orifice flow $\dot{w}_o$ and blade flow $\dot{w}_b$ found during the blade bench flow calibrations indicates that the flow disturbances in the base of the nonrotating blades are not a great problem. Furthermore, when the blade was operated in the spin rig to speeds of 9000 rpm, there was only a 10 percent maximum deviation in these flow data from the correlation line (fig. 10). The flow dis-

turbance effects are obviously less than 10 percent because the total deviation may be attributed partially to other experimental uncertainties. A discussion of these uncertainties is presented in the next section.

Data Scatter

The small scatter, ±10 percent of the flow data presented in figure 10, indicates that this rotating flow measuring system is practical. The discussion in this section covers some of the experimental uncertainties associated with the data spread. These uncertainties (errors) arise as a result of lack of perfect precision in the measuring instruments, lack of achieving perfect steady-state conditions and difficulties in constructing perfectly precise mathematical models needed to analyze the experiment.

Random pressure fluctuations in the cooling air system (about 1 percent) and measurement error incurred during the orifice calibration (1 percent) produced a maximum error in $\dot{w}_o$ of about 2 percent. The maximum error in $\dot{w}_b$ was about 8 percent and was due to uncertainties in the value of the calibrated effective area α used in equation (6) (about 3 percent as represented by the scatter of the data about the least-square line presented in fig. 9), random supply pressure fluctuations (1 percent) and transducer system (including slip rings) measurement error (1 to 4 percent) as speed was varied from 0 to 9000 rpm. These maximum uncertainties can approximately account for the 10 percent maximum deviation of the spin rig data from the least-square line (fig. 10).

Included in the uncertainties in transducer system measurement error are (1) the effects of transducer characteristics such as hysteresis and linearity on transducer performance; (2) the lack of precision involved in the assumption that the temperature values obtained with the stationary reference thermocouple could be used for T_5 (fig. 4); (3) the assumption (needed in the model used to obtain eq. (1)) of no temperature gradient along the air columns contained within the pressure tubing from the blade. With regard to the first of these uncertainties, analysis of the transducer characteristics (hysteresis and linearity) obtained from the stationary spin rig calibration indicated that transducer experimental error would affect values of $\dot{w}_b$ by less than 1/2 percent. It was assumed that these characteristics did not change during rotational conditions. A highly accurate measurement of T (the second uncertainty) was not necessary; the exponential quantity in equation (1) (corresponding to the calculation of p_A, which involves use of T_5) was at most 1.004 over the range of speeds of 0 to 9000 rpm and temperatures of 300 to 456 K (80° to 360° F).

Concerning the third uncertainty, temperature gradients in the air contained within the tubes can arise from compression and frictional heating due to rotation of the disk and tubes. A rough evaluation of the temperature gradient uncertainty was made by

considering the additive and independent effects of compression and frictional heating on $\dot{w}_b$. Calculations show that gradients arising from compression alone will lead to a maximum uncertainty in $\dot{w}_b$ of about 1 percent at 9000 rpm. During frictional heating, an air layer adjacent to the disk is carried by it through friction and is thrown radially outward due to the action of centrifugal forces. Calculations using the rotating disk model presented in reference 7 indicate that the pressure sensing tubes (on the disk) and the stationary spin rig thermocouple located at 26.7 centimeters (10.5 in.) radius lay within the effected air layer. This flowing air layer will absorb the frictional heat, setting up a radial temperature gradient in it and in the air contained in the tubes. At maximum speed, the indicated temperatures from the stationary thermocouple and from the rotating tubing thermocouple T_6 agreed within 6 K (11° F). This temperature gradient would result in a maximum uncertainty in $\dot{w}_b$ of less than 1/2 percent. Thus, the total additive error in $\dot{w}_b$ is about $1\frac{1}{2}$ percent which indicates that the assumption of no temperature gradient is reasonable for these tests.

SUMMARY OF RESULTS

The performance of a rotating flow measurement system which measured the air mass flow rate in the coolant passages of a turbine blade was investigated at speeds from 0 to 9000 rpm. Mass flow rates ranging from about 0.0035 to 0.039 kilogram per second (0.0077 to 0.085 lbm/sec) at air temperatures of 300 to 385 K (80° to 233° F) were determined with pressure instrumentation installed in the blade base region of the rotating blade. The important results of the investigation are summarized as follows:

1. A single calibrated effective area could be used in a conventional flow equation to determine the air mass flow rate through the blade base for all rotative speeds and mass flows investigated.

2. Individual rotating flow measurements of blade mass flow rates agreed with corresponding stationary flow measurements using a calibrated reference orifice within 10 percent at shaft speeds from 0 to 9000 rpm.

Lewis Research Center,
National Aeronautics and Space Administration,
Cleveland, Ohio, March 11, 1974,
501-24.

REFERENCES

1. Pollack Frank G.; Liebert, Curt H.; and Peterson, Victor S.: Rotating Pressure Measuring System for Turbine Cooling Investigations. NASA TM X-2621, 1972.

2. Calvert, Howard F.; Cochran, Reeves P.; Dengler, Robert P.; Hickel, Robert O.; and Norris, James W.: Turbine Cooling Research Facility. NASA TM X-1927, 1970.

3. Poferl, David J.; Svehla, Roger A.; and Lewandowski, Kenneth: Thermodynamic and Transport Properties of Air and the Combustion Products of Natural Gas and of ASTM-A-1 Fuel with Air. NASA TN D-5452, 1969.

4. Zuk, John; Ludwig, Laurence P.; and Johnson, Robert L.: Design Study of Shaft Face Seal with Self-Acting Lift Augmentation. I - Self-Acting Pad Geometry. NASA TN D-5744, 1970.

5. Bean, Howard, ed.: Fluid Meters: Their Theory and Application. 6th edition, American Society of Mechanical Engineers, 1971.

6. Ito, H.; and Nanba, K.: Flow in Rotating Straight Pipes of Circular Cross Section. Jour. Basic Engineering, Sept. 1971, pp. 383-393.

7. Schlichting, Hermann (J. Kestin, trans.): Boundary Layer Theory. 6th edition, McGraw-Hill Book Co., Inc., 1968.

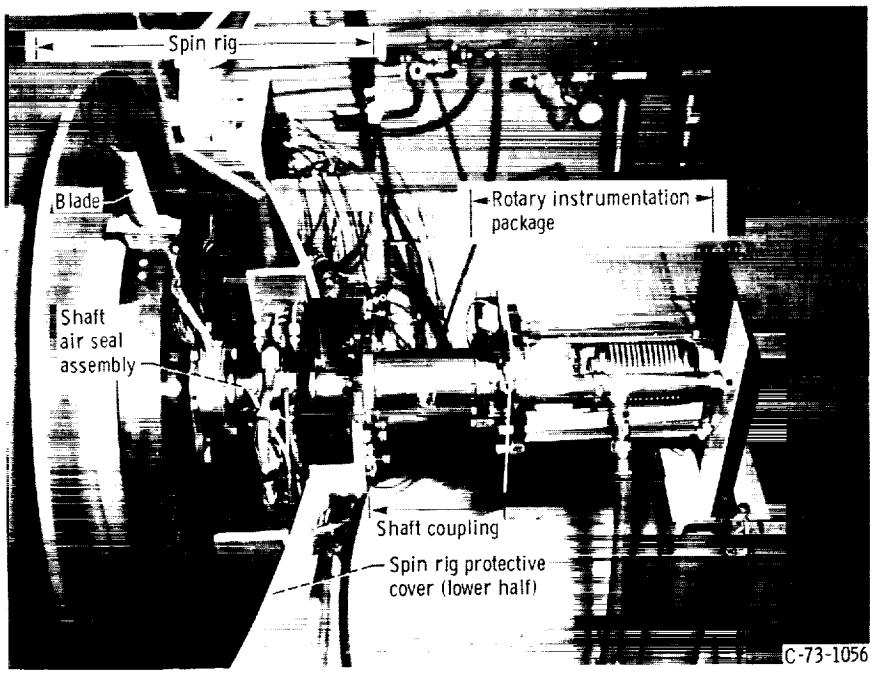

Figure 3. - Spin rig and other attached components.

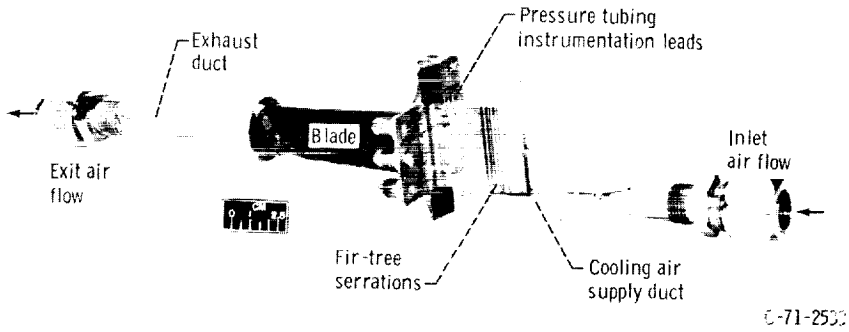

Figure 1. - Blade assembly for stationary bench flow tests.

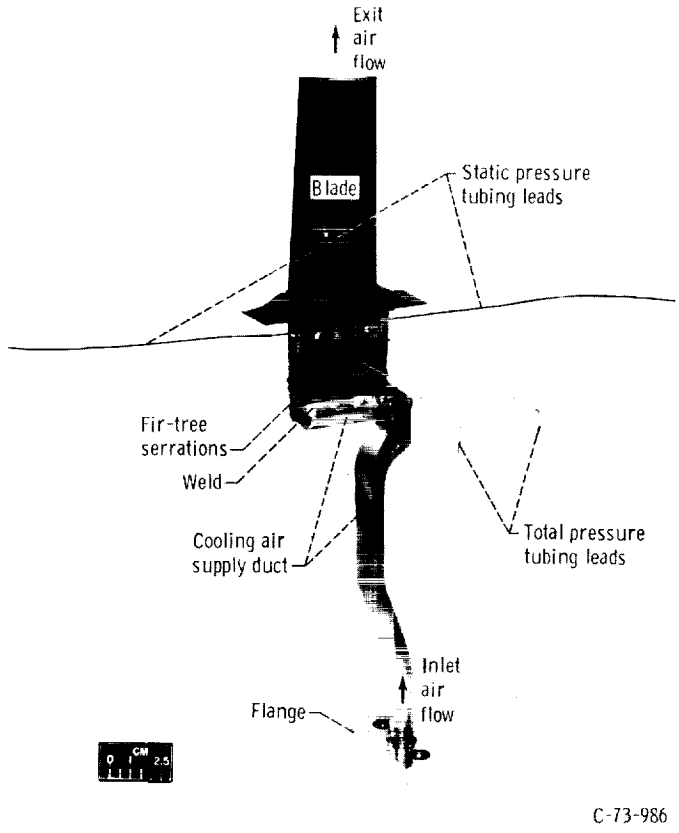

Figure 2. - Blade assembly for spin rig tests.

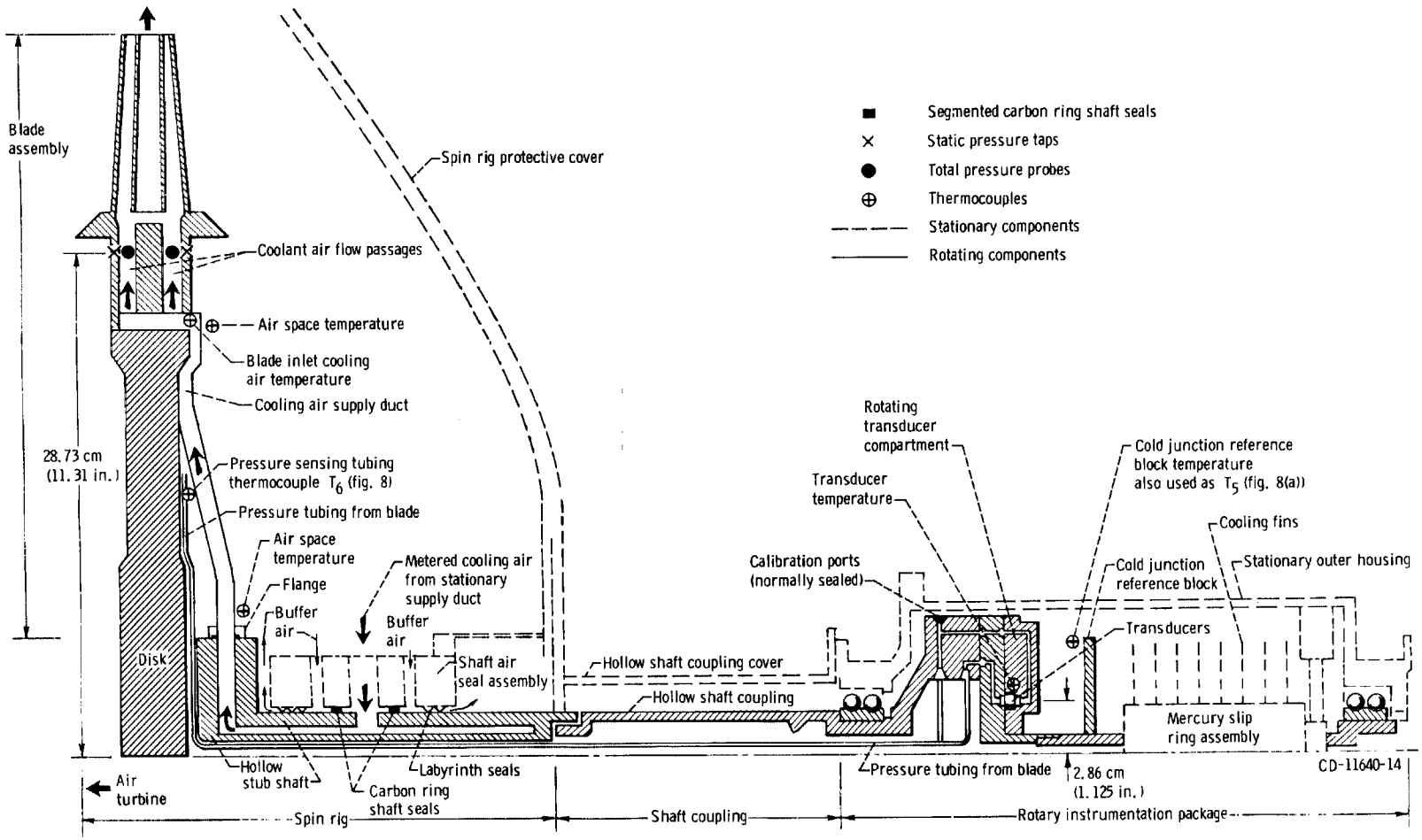

Figure 4. - Schematic of spin rig and other attached components.

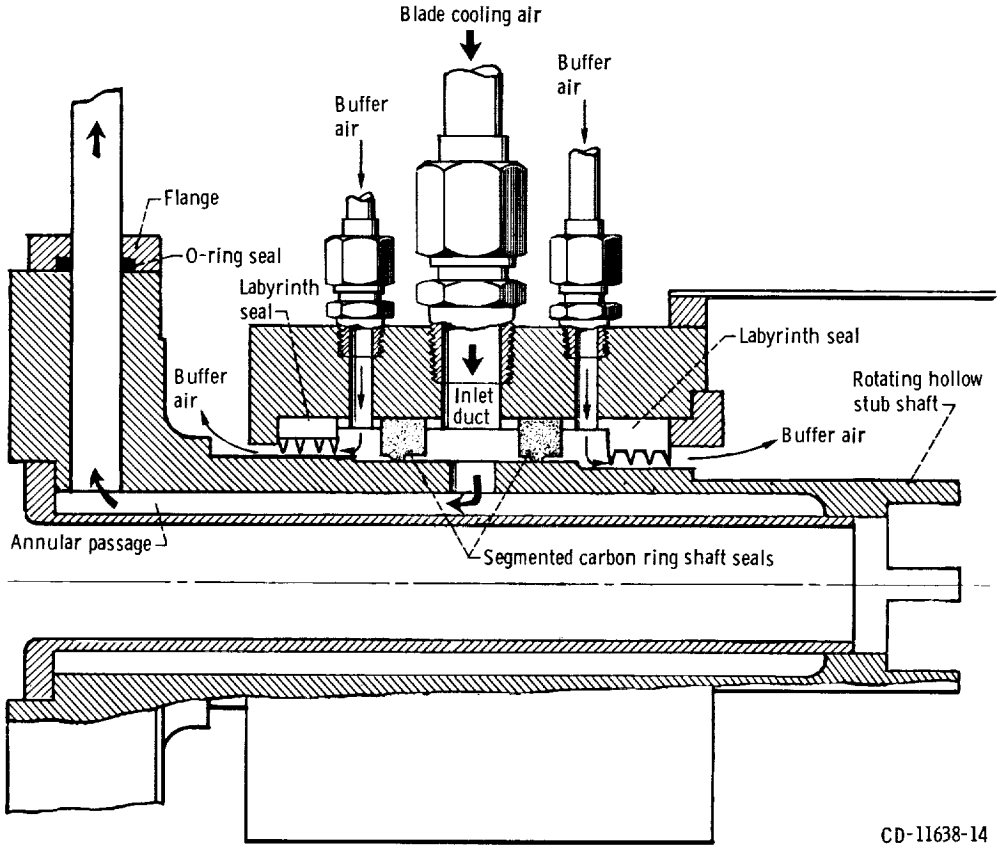

Figure 5. - Cross-sectional diagram of shaft air seal assembly.

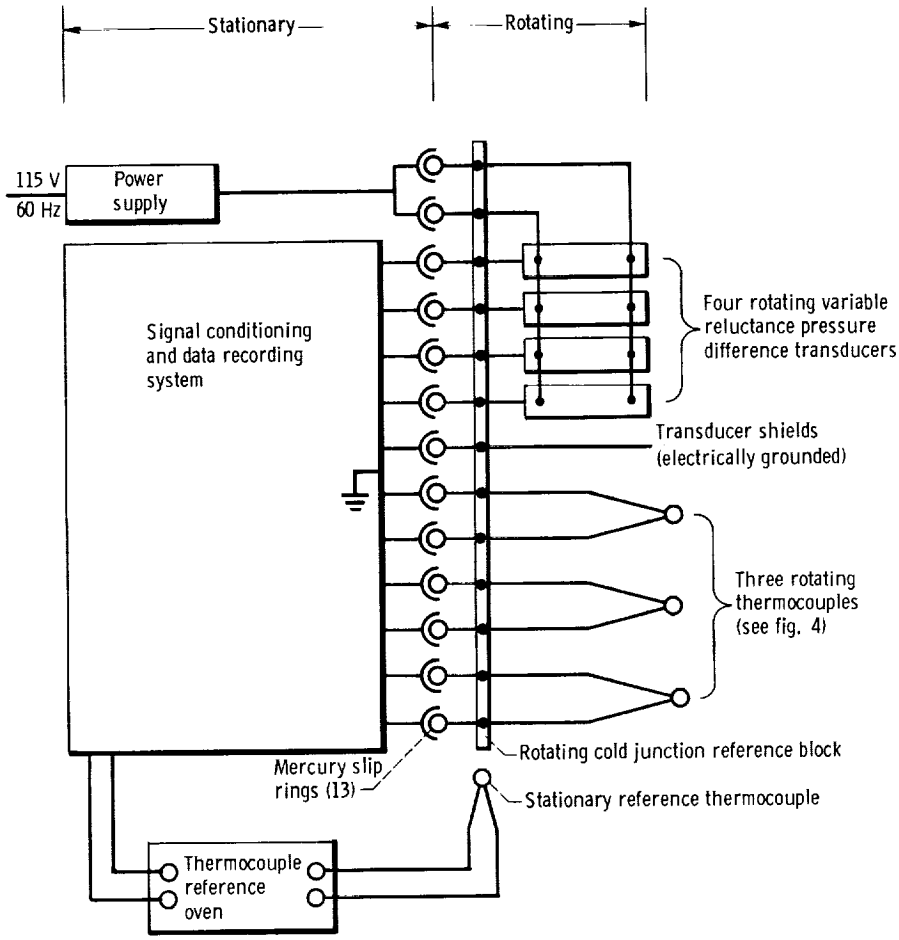

Figure 6. - Block diagram of rotating pressure and temperature measurement system.

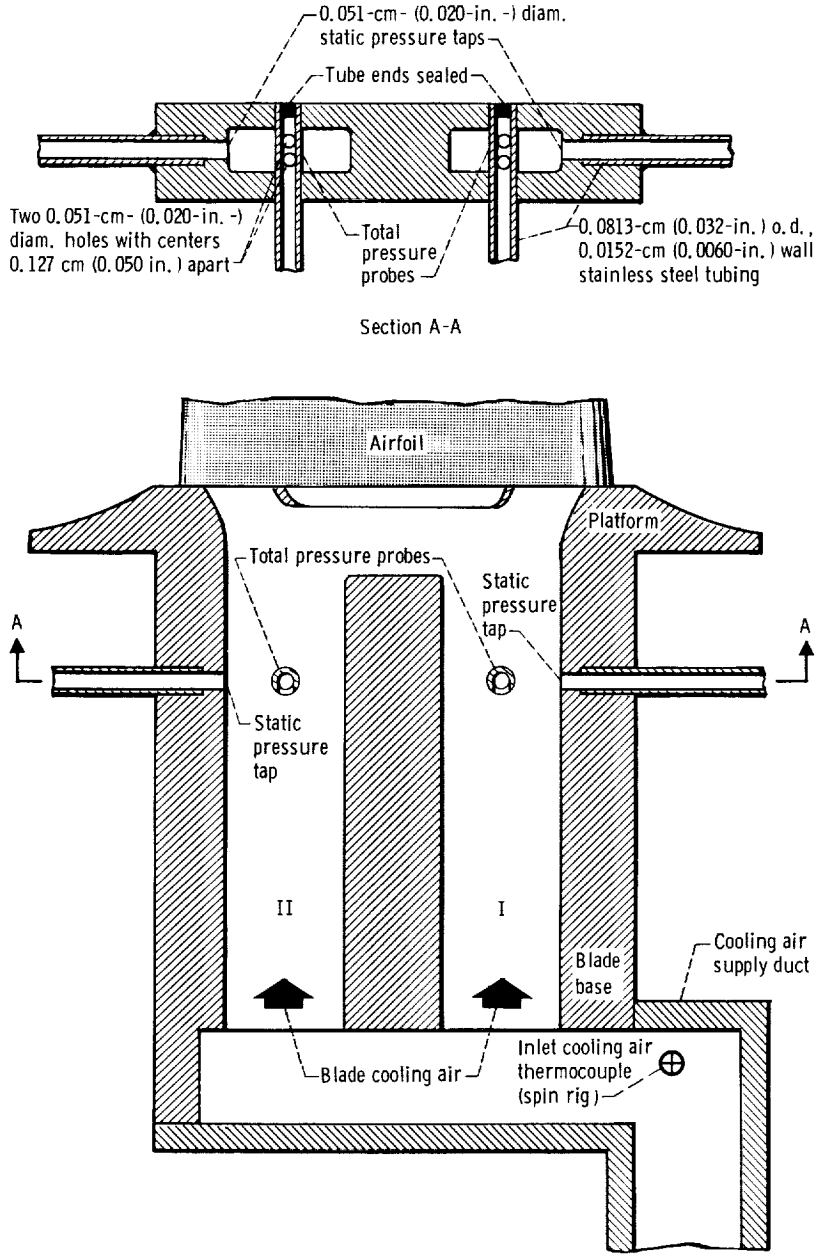

Figure 7. - Blade instrumentation (not to scale). CD-11639-14

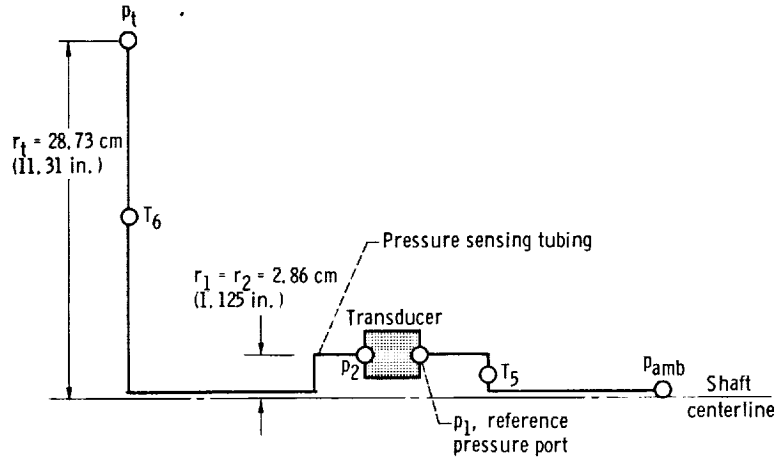

(a) Total-ambient pressure difference.

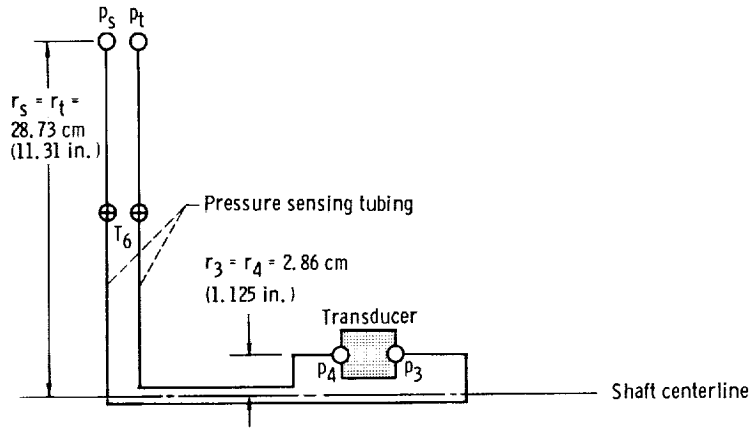

(b) Total-static pressure difference.

Figure 8. - Schematic of instrumentation location in spin rig tests.

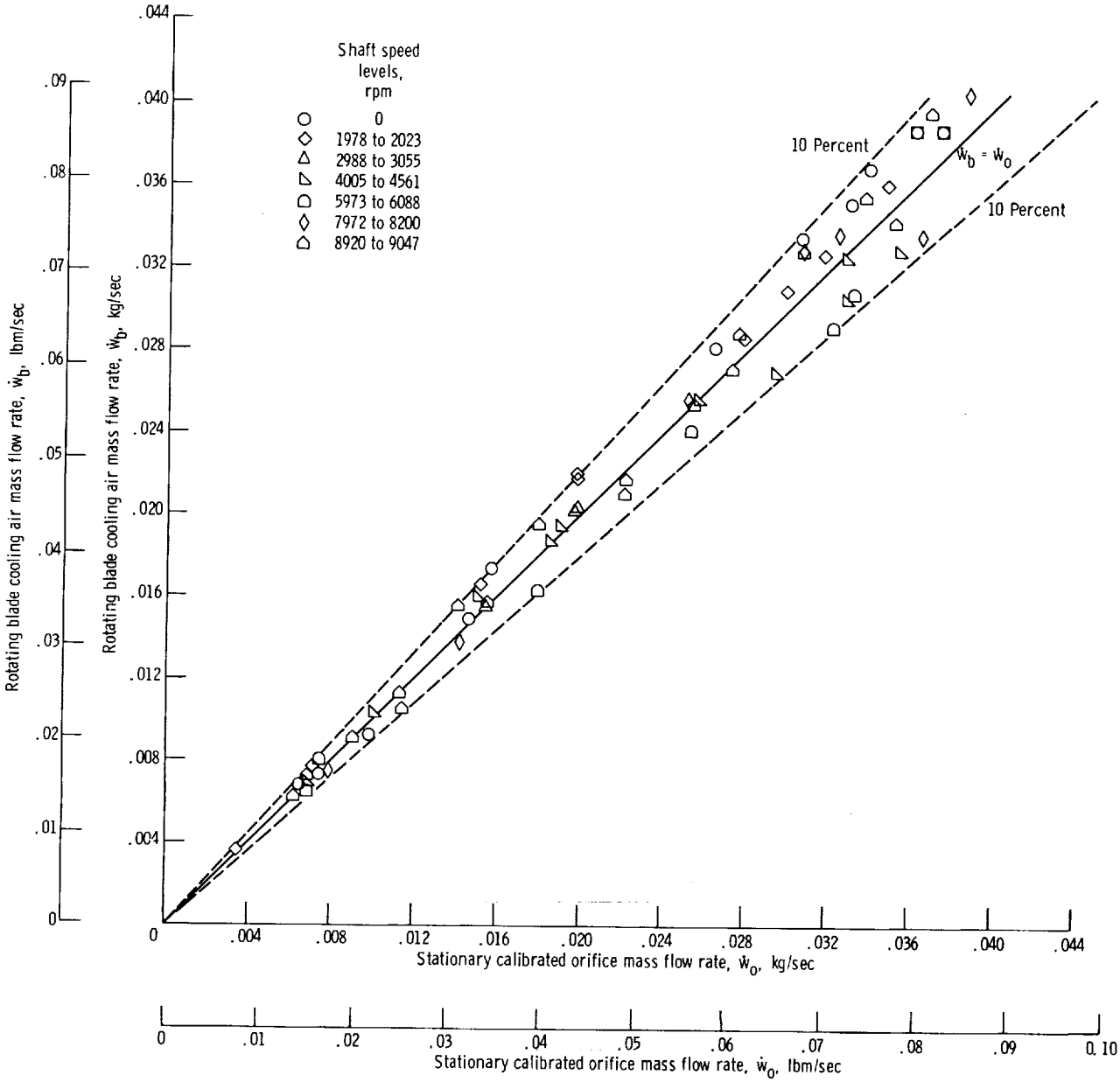

Figure 10. - Comparison of rotating blade airflow rates and stationary calibrated orifice airflow rates in spin rig tests. (Sixty-seven data points.)

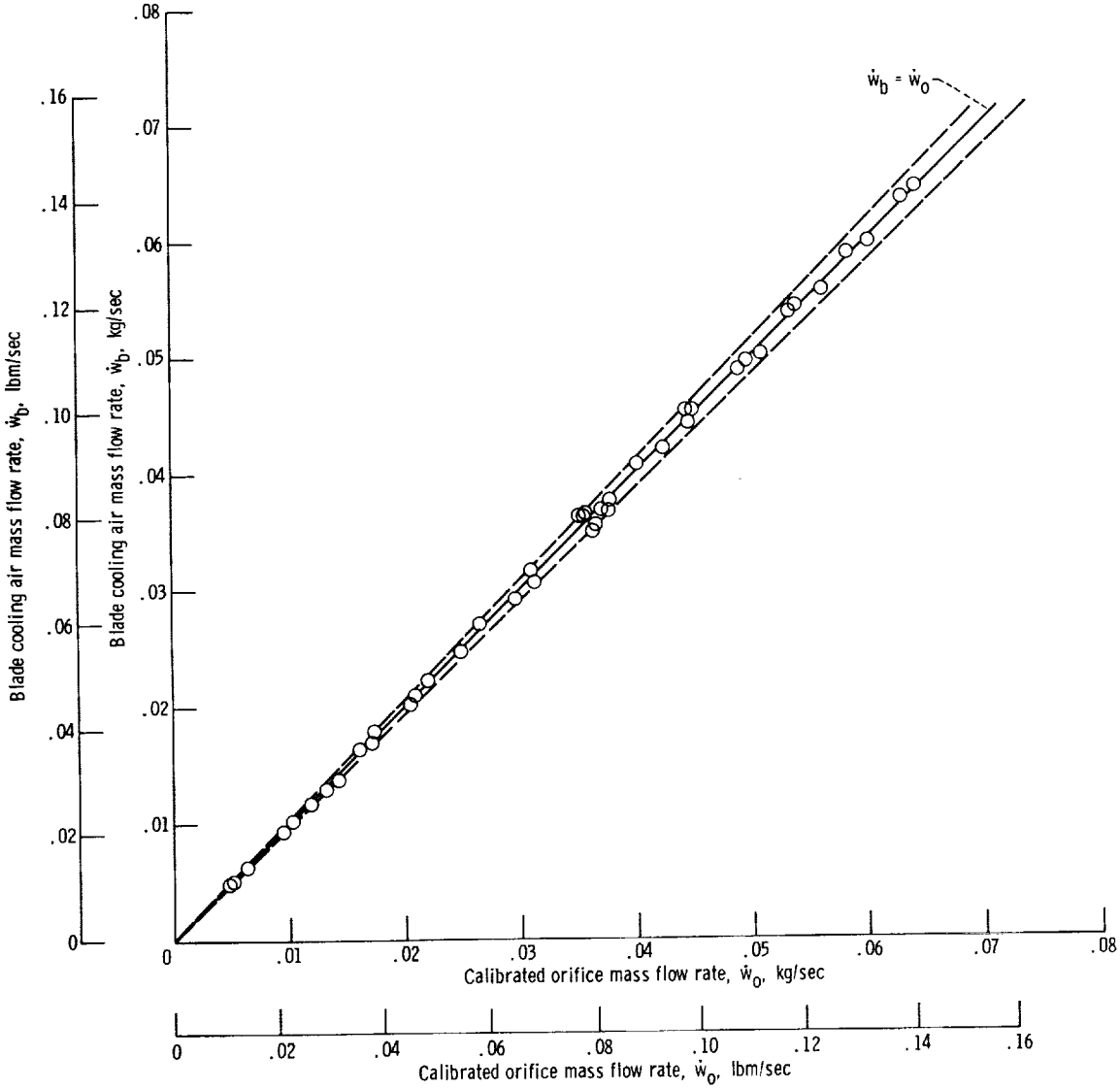

Figure 9. - Comparison of blade airflow rates and calibrated orifice airflow rates in stationary bench flow test. Calibrated effective area α, 0.316 square centimeter (0.0490 in.^{2}). (Forty-seven data points.)